

SMART VISION SENSOR FOR VELOCITY ESTIMATION USING A MULTI-RESOLUTION ARCHITECTURE

Mickael Quelin, Abdesselam Bouzerdoum and Son Lam Phung

ICT Research Institute, University of Wollongong, Northfields Avenue, NSW 2522 Wollongong, Australia

Keywords: Insect vision, Multi-resolution architecture, Elementary Motion Detector (EMD), Elementary Velocity Detector (EVD), Horridge template model, Reichardt correlator.

Abstract: This paper presents a velocity estimator based on a digital version of the so called Elementary Motion Detector (EMD). Inspired by insect vision, this model benefits from a low complexity motion detection algorithm and is able to estimate velocities in four directions. It can handle noisy images with a pre-filtering step which highlights the important features to be detected. Using a specific velocity tuned detector called Elementary Velocity Detector (EVD) applied to different resolutions of the same input, it gains time efficiency by estimating different speeds in parallel. The responses of the different EVDs are then combined together at the input resolution size.

1 INTRODUCTION

In computer vision, motion detection is considered to be an important cue for interpreting the visual field and recovering the environment structures. Methods to measure image motion are numerous and classified in two main categories which are the intensity-based methods, including the correlation and gradient models, and the token-based methods for long-range motions (Sarpeshkar et al., 1996). Recently, new evaluation methods have been proposed to compare and improve the latest optical flow estimator (Baker et al., 2007). Computer vision systems are today considered to be a promising technology for improving vehicle safety, therefore low complexity and fast processing algorithms are needed to build such real-time systems.

Insect-based vision systems have been investigated for many years. The size of insects brains and bodies suggests a simple neural system which contributes to the fast processing of information. It is therefore an interesting method to investigate in order to design real-time applications. Proposed in the 1950's, the Reichardt model (Hassenstein and Reichardt, 1956) is an asymmetric non-linear correlator, which has formed the basis of many models. Often referred to as the Elementary Motion Detector (EMD), its accuracy, reliability and limitation to estimate velocity of motions have been discussed (Dror et al., 2001). More recent models also successfully im-

proved its performance in velocity estimation (Zanker et al., 1999; Riabinina and Philippides, 2009). Netter, Franceschini and Iida et al. (Netter and Franceschini, 2002; Iida and Lambrinos, 2000) successfully used several EMDs to build odometers and distance measurement tools. The results of their experiments in a confined environment led to efficient applications in micro air vehicle (MAV) navigation control. Other higher level architectures managed to deal with image video inputs by combining several EMDs to build array architectures. Jun and his co-workers (Jun et al., 2004) proposed a moving object detection architecture, whereas other authors (Tianguang et al., 2008; Nakamura et al., 2002) characterized motion direction or nature of motion respectively. Furthermore Harrison (Harrison, 2005) achieved a simple collision detector using a radially orientated EMD architecture which does not need other post processing than adding and thresholding the EMDs outputs. Those models prove that the understanding of insect vision goes through the design of specific efficient applications which can be realized without the need for accurate directional and velocity information.

Proposed in the early 1990's, the template model (Horridge, 1990) simplifies the Reichardt model in order to be implemented with digital hardware. That is why we use this promising technique for our work.

However one common problem to all those models is adaptation of the EMD to change in contrast and

luminance. They commonly deal with this issue by using a filter to remove the DC component of the input signal. This reduces the effect of luminance changes.

In this paper we propose a new model to estimate motion velocities on stationary camera videos which might be used for non-stationary ones. Firstly, the principle of the template model is reviewed. In Section 3, we extend this model to process two-dimensional (2D) video images and therefore build a four-directional motion detector. To make this model more robust to noise, and achieve a clearer response to the input signal, a pre-filtering step with the simulation and real-time results of the motion detector is presented in Section 4. Section 5 describes our Elementary Velocity Detector (EVD) principle and its results. This one uses an original velocity tuned detection which is implemented at different resolutions of the input to be able to process a wider range of speeds. Finally, this paper concludes with some outcomes.

2 TEMPLATE MODEL

The template model belongs to the spatiotemporal correlator scheme. As the Reichardt detector, it is directionally sensitive. It can simply be seen as a digital version of the Reichardt EMD. It is an empirical model which extracts, from intensity jump, an indicator of directional motion.

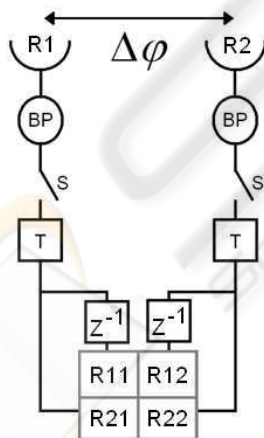


Figure 1: Template model scheme. R1 and R2: Photoreceptors, BP: Bandpass filter, T: Threshold function, S: Switch, z^{-1} : Delay function, $\Delta\phi$: Spatial period.

Figure 1 presents the EMD of the template model. The visual field is spatially and temporally sampled. The symbol $\Delta\phi$ is the distance or spatial period between the photoreceptors. A band-pass (BP) filter

Table 1: List of motion templates.

Polarity	Motion to right		Motion to left	
	code	Template	code	Template
Dark-to-bright	A	$\begin{bmatrix} +1 & 0 \\ +1 & +1 \end{bmatrix}$	E	$\begin{bmatrix} 0 & +1 \\ +1 & +1 \end{bmatrix}$
	B	$\begin{bmatrix} +1 & +1 \\ 0 & +1 \end{bmatrix}$	F	$\begin{bmatrix} +1 & +1 \\ +1 & 0 \end{bmatrix}$
Bright-to-dark	C	$\begin{bmatrix} -1 & 0 \\ -1 & -1 \end{bmatrix}$	G	$\begin{bmatrix} 0 & -1 \\ -1 & -1 \end{bmatrix}$
	D	$\begin{bmatrix} -1 & -1 \\ 0 & -1 \end{bmatrix}$	H	$\begin{bmatrix} -1 & -1 \\ -1 & 0 \end{bmatrix}$

produces information on changes in the input which is sampled by a switch. A threshold function then splits it into 3 states: -1 if the intensity is decreasing, +1 if it is increasing, 0 otherwise. The current states of the two channels are transmitted to the bottom row of the 2-by-2 output matrix and the previous states (defined by a delay z^{-1}) are transmitted to the first row of the matrix.

Over the 81 possible matrices or templates of size 2-by-2, 8 of them indicate the existence of motion to a specific direction (from one receptor to another). Information about the polarity of the edge transition as well as beginning and ending of the phenomenon is also coded as shown in Table 1 (Nguyen et al., 1996).

Thus, this detector is sensitive to direction and polarity. It gives a simple and easy implementation model for digital hardware. However the threshold value has a significant influence on the output and its optimum value depends on changes in contrast and luminance of the input signal. Also, the velocity sensitivity of the Reichardt model as studied by Dror (Dror et al., 2001) is lost here by digitizing the output into 3 states. Moreover, the spatial distance between associated templates, such as templates E and F or A and B which code the beginning and ending of a transition, depends on both the spatial length of the transition and the velocity of the motion. Therefore it cannot be used in the estimation of the velocity without extra information. However Nguyen et al. proposed a tracking algorithm to get velocity with this model as described in Section 5.

3 HANDLING VIDEO INPUTS

Using the template model to process 2D frames of a video input requires the definition of the spatiotemporal sampling of the EMD and the extension of the

one-dimensional (1D) direction sensitivity to 2D direction sensitivity.

In order to retain all the details that the input signal provides, it is logical to match the input spatiotemporal resolution to the EMD. Therefore, we choose $\Delta\phi$ as the distance between two pixels and z^{-1} as the frame rate of the video. The filter is here implemented as a high-pass (HP) filter by simply subtracting the previous intensity input from the current one and thus having the sign of the filter output coding the evolution of the intensity.

To detect all kinds of motion in the video, it is often proposed to combine two EMD architectures in an orthogonal fashion such as sensing the x and y directions so that motion in all directions can be reconstructed. Jun et al. and Tianguang et al. proposed two 2D EMDs using a 4-pixel X or 3-pixel Γ shape respectively (Jun et al., 2004; Tianguang et al., 2008). The association of motion to the output they proposed is not completely consistent in terms of location. Here we propose another 5-pixel + shape EMD which has the advantage of linking motions to the starting point which is an actual pixel position in the input frame (see Fig. 2c).

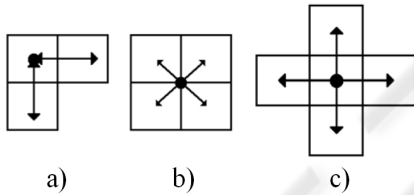


Figure 2: EMD architectures. The dots represent location to where motions detected are linked. a) Γ , b) X, c) +.

4 FILTER AND MOTION DETECTION RESULTS

Because of the threshold adjustment and to make the sensor more robust to noise and sensitive to motion, a filter has been applied to the input video. A combination of a Gaussian filter and Sobel operator which we refer to here as the "Gaubel" filter will remove noise and highlight edges. Equation (1) presents the "Gaubel" filter we designed,

$$I_{out} = \sqrt{[(S_x * G) * I_{in}]^2 + [(S_y * G) * I_{in}]^2} \quad (1)$$

where I_{in} is the input image, S_x and S_y are the 3-by-3 Sobel kernels for horizontal and vertical changes, G is the Gaussian smoothing window and $*$ is a convolution operator.

The standard deviation of the Gaussian equals to 1/6 of the window size in order to produce a consistent smoothing. Normalizing the Gaussian also limits the range of contrast and luminance at the output and facilitates the threshold adjustment. The final image is obtained by calculating the gradient. Figure 3 shows the result of the application of the filter on a noisy image.

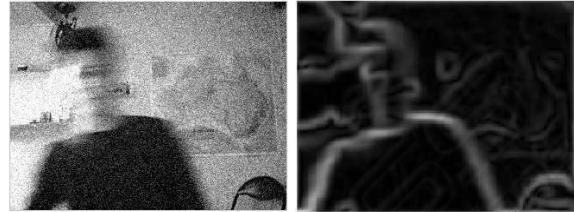


Figure 3: Filtered input. left: noisy input image, right: filtered image.

The threshold is adjusted to be sufficiently large, to be sensitive to changes of intensity of moving edges and to avoid detecting noise. By testing several Gaussian window sizes (see Fig. 4), a balance can be found to remove noise (increasing the size) and keep motion locations as precise as possible (decreasing the window size). Finally, it is worth noting that using an edge detection operator gives more features to detect.

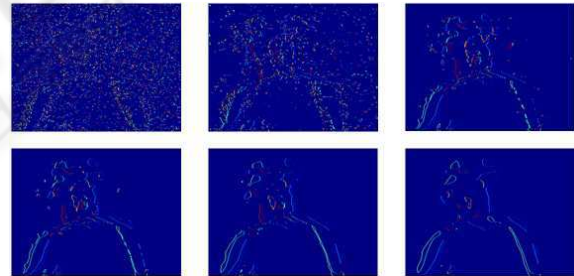


Figure 4: Output of the motion detector with filtered input for different Gaussian window sizes. Only left and right motion direction templates are displayed in color-coded format. The only moving object in the input is the body moving from left to right. The window sizes used, from left to right top to bottom are 7, 11, 17, 21, 27 and 37.

A test of the motion detector in real-time has been realized. Using a smaller Gaussian window size in order to increase the processing time of each frame, led to a noisy output as all frames cannot be handled at a rate of 20 *fps* (see Fig. 5).



Figure 5: Real-time implementation. A code templates are displayed in the output. Only the hand is moving to the right direction. left: input image, middle: filtered image, right: output of the motion detector.

5 ELEMENTARY VELOCITY DETECTOR

Use of the template model for velocity estimation has been realized in the past by tracking templates and linking them over space and time (Nguyen et al., 1996). The search space defined directly governs the velocity range that the estimator is able to track. Such a method gives an accurate estimation but as the tracking process depends on the searching step and on the number of features to track, it is impossible to determine how long the algorithm will take to process an unknown input. This phenomenon would be even worse if dealing with video inputs. Because the proposed system aims to be implemented in real-time, we need a solution which uses a defined time to process any input frame.

5.1 Template for Velocity

To be able to estimate velocity, the matching of at least two templates in space and time needs to be achieved. In order to remove any tracking process or search space, we have designed a new family of velocity dependent templates. Those are obtained by linking two motion templates in space and time to generate 8 new ones as described in Table 2. To achieve such a match the elementary detector needs to be reviewed by implementing an extra photoreceptor in the fashion described in Fig. 6.

The new velocity templates are made out of 3-by-3 matrices with the top row generated by an extra delay. This means that our new features are only able to match motion templates (of same code) over one pixel space difference and one frame temporal difference. In other words, this architecture is sensitive to an elementary velocity of one pixel per frame (1 *ppf*).

We also have extended the elementary detector architecture to be able to process video inputs. The Elementary Velocity Detector (EVD) is shown in Fig. 7. This one keeps the advantages of our EMD in terms

Table 2: List of velocity templates.

Polarity	Motion to right		Motion to left	
	code	Template	code	Template
Dark-to-bright	A	$\begin{bmatrix} +1 & 0 & - \\ +1 & +1 & 0 \\ - & +1 & +1 \end{bmatrix}$	E	$\begin{bmatrix} - & 0 & +1 \\ 0 & +1 & +1 \\ +1 & +1 & - \end{bmatrix}$
	B	$\begin{bmatrix} +1 & +1 & - \\ 0 & +1 & +1 \\ - & 0 & +1 \end{bmatrix}$	F	$\begin{bmatrix} - & +1 & +1 \\ +1 & +1 & 0 \\ +1 & 0 & - \end{bmatrix}$
Bright-to-dark	C	$\begin{bmatrix} -1 & 0 & - \\ -1 & -1 & 0 \\ - & -1 & -1 \end{bmatrix}$	G	$\begin{bmatrix} - & 0 & -1 \\ 0 & -1 & -1 \\ -1 & -1 & - \end{bmatrix}$
	D	$\begin{bmatrix} -1 & -1 & - \\ 0 & -1 & -1 \\ - & 0 & -1 \end{bmatrix}$	H	$\begin{bmatrix} - & -1 & -1 \\ -1 & -1 & 0 \\ -1 & 0 & - \end{bmatrix}$

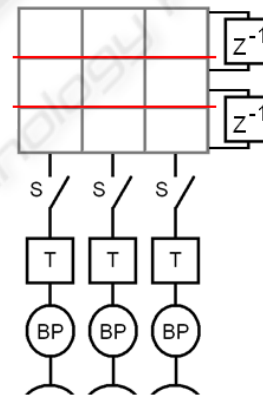


Figure 6: Velocity template model Scheme.

of linking the velocity to the starting point which is an actual pixel in the input frame. Finally, the direction of velocity motion is coded with colors. The output color code is as follows: right direction velocities are displayed in red color, up in purple, down in yellow, left in cyan, down and right in orange, up and right in pink etc.

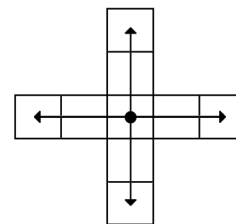


Figure 7: EVD architecture.

5.2 Multi-Resolution Velocity Estimation Architecture

The EVD model provides a tool to estimate directional velocities of an entire video frame with a fixed processing time. However it has one main disadvantage in terms of the range of velocities detected. In order to use the same EVD to estimate other velocities, a multi-resolution architecture is set up (see Fig. 8 below).

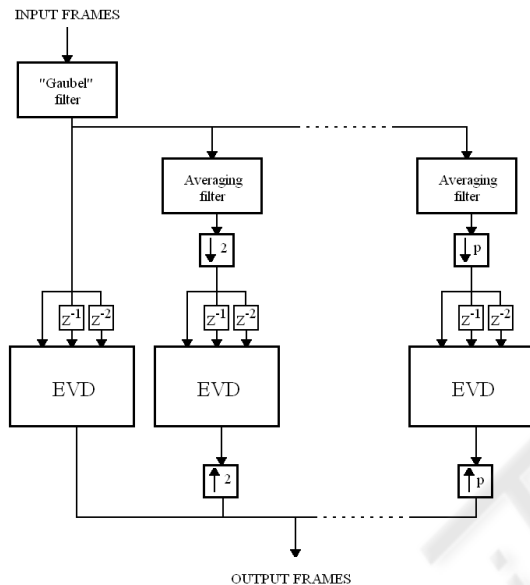


Figure 8: Multi-Resolution Architecture Scheme.

The frames are processed by the "Gaubel" filter and then transmitted to each resolution channel to be processed in parallel. To lower the resolution of the input, an averaging filter is implemented in each channel. The convolution kernel size used is related to the channel resolution. Then each averaged image is sub-sampled to obtain the channel resolution. In order to detect the velocity templates, three consecutive frames are needed. Two delays are therefore implemented in front of the EVD. The presence of velocity templates is then checked by the EVD for each pixel and the output image is produced. This leads to one image for each resolution processed. Finally, to group all these results in one final frame, lower resolutions are up-sampled to match the original input frame size and are all combined together. The up-sampling is simply realized by expanding each pixel to its surrounding area.

By using the EVD on a lower resolution input, a higher velocity can be estimated. For example, a velocity of 2 ppf at a M -by- N resolution will be estimated as being 1 ppf at a resolution of $M/2$ -by- $N/2$

and therefore will be sensed by the EVD. Thus velocity from 1 ppf and higher can theoretically be estimated by this architecture.

A characteristic of this model which can be considered as an advantage is that higher velocities are represented by bigger squares in the combined output.

5.3 Results

Figures 9 to 11 display results of the final multi-resolution architecture using 4 different resolutions. All the results were produced using the same input video which displays a hand accelerating to the right direction.

In Figure 9, the EVD processing the original resolution divided by two is the one displaying more templates. This means that according to the detector, the hand is moving at around 2 ppf . In Figure 10 the hand appears to be moving at around 3 ppf (features mainly detected at 2 ppf and 4 ppf) and in Figure 11 at around 6 ppf . Based on the fact that figures are sorted in chronological order, these results are consistent, considering that the hand is actually accelerating.

By bringing outputs together, we can see that almost the entire object edges are displayed, this despite detection of the entire range of velocities is not implemented (3 ppf , 5 ppf , 6 ppf etc.).

An advantage of this architecture is the ability to estimate a global object motion velocity using information on each resolution processed by the EVD, meanwhile keeping all velocity components of the object, such as a finger moving independently from the hand.

6 CONCLUSIONS

In this paper, an insect vision based motion detection technique has been extended to velocity estimation. A filter has been used to make it more robust and responsive to moving edges. We also have introduced the concept of the Elementary Velocity Detector using velocity templates. This one has been implemented on a multi-resolution architecture and has been successfully tested. The simulations and experiments demonstrate that this elaborated model produces consistent and promising results. Thus, this simplistic insect inspired algorithm, ideal for parallel computing, provides information exploitable for specific applications without need for precise directional and velocity information. However as we are willing to use more realistic video inputs, i.e. complex backgrounds

or moving cameras, a further adaptation to change in contrast and luminance would be required.

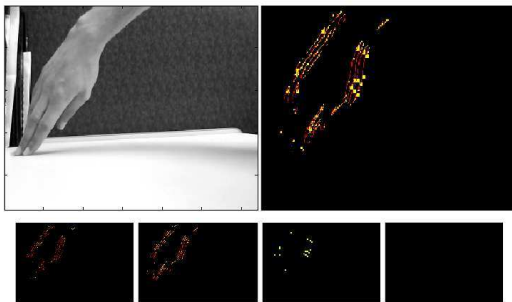


Figure 9: Example of input and outputs of the EVD architecture. top left: input frame, top right: final output, bottom left: output at original resolution, bottom middle left: output at original resolution/2, bottom middle right: output at original resolution/4, bottom right: output at original resolution/8.

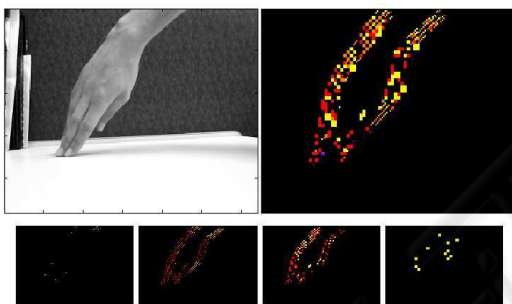


Figure 10: Example of input and outputs of the EVD architecture. top left: input frame, top right: final output, bottom left: output at original resolution, bottom middle left: output at original resolution/2, bottom middle right: output at original resolution/4, bottom right: output at original resolution/8.

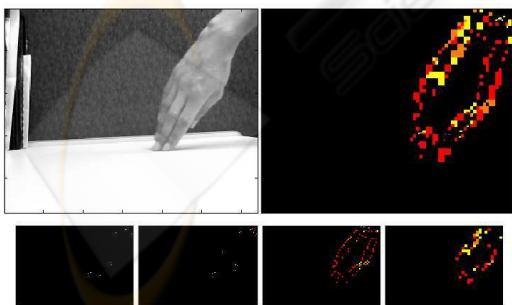


Figure 11: Example of input and outputs of the EVD architecture. top left: input frame, top right: final output, bottom left: output at original resolution, bottom middle left: output at original resolution/2, bottom middle right: output at original resolution/4, bottom right: output at original resolution/8.

REFERENCES

- Baker, S., Scharstein, D., Lewis, J., Roth, S., Black, M., and Szeliski, R. (2007). A database and evaluation methodology for optical flow. In *Proceedings of the IEEE Int. Conf. Computer Vision*, pages 1–8.
- Dror, R. O., O'Carroll, D. C., and Laughlin, S. B. (2001). Accuracy of velocity estimation by reichardt correlators. *J. Opt. Soc. Am. A*, 18(2):241–252.
- Harrison, R. R. (2005). A biologically inspired analog ic for visual collision detection. *IEEE Trans. Circuits Syst. Regul. Pap.*, 52(11):2308–2318.
- Hassenstein, B. and Reichardt, W. (1956). Functional structure of a mechanism of perception of optical movement. In Rosenblith, W. A., editor, *Proc. Int. Cong. Cybern.*, pages 797–801, Namur.
- Horrige, G. A. (1990). A template theory to relate visual processing to digital circuitry. In *Proc. R. Soc. Lond.*, volume Vol. B 239, pages 17–33.
- Iida, F. and Lambrinos, D. (2000). Navigation in an autonomous flying robot by using a biologically inspired visual odometer. In *Proc. SPIE Sensor Fusion and Decentralized Control in Rob. Syst. III*, volume Vol. 4196, pages 86–97.
- Jun, Y., Dong-Guang, L., Hui-Min, F., and Zhi-Feng, L. (2004). Moving objects detection by imitating biologic vision based on fly's eyes. In *Proc. ROBIO 2004 IEEE Int. Conf. Rob. and Biomim.*, pages 763–766.
- Nakamura, E., Ichimura, M., and Sawada, K. (2002). Fast global motion estimation algorithm based on elementary motion detectors. In *Proc. 2002 Int. Conf. Image Processing*, volume 2, pages II–297–II–300 vol.2.
- Netter, T. and Franceschini, N. (2002). A robotic aircraft that follows terrain using a neuromorphic eye. In *Proc. IEEE/RSJ Int. Conf. Intel. Rob. and Syst.*, volume 1, pages 129–134 vol.1.
- Nguyen, X., Bouzerdoum, A., and Bogner, R. (1996). Backward tracking of motion trajectories for velocity estimation. In *Proc. 1996 Australian and New Zealand Conf. Intelligent Information Systems*, pages 338 – 341.
- Riabinina, O. and Philippides, A. O. (2009). A model of visual detection of angular speed for bees. *J. Theor. Biol.*, 257(1):61–72.
- Sarpeshkar, R., Kramer, J., Indiveri, G., and Koch, C. (1996). Analog vlsi architectures for motion processing: from fundamental limits to system applications. In *Proc. IEEE*, volume 84, pages 969–987.
- Tianguang, Z., Haiyan, W., Borst, A., Kuhnlenz, K., and Buss, M. (2008). An fpga implementation of insect-inspired motion detector for high-speed vision systems. In *Proc. IEEE Int. Conf. Rob. and Autom.*, pages 335–340.
- Zanker, J. M., Srinivasan, M. V., and Egelhaaf, M. (1999). Speed tuning in elementary motion detectors of the correlation type. *Biol. Cybern.*, 80(2):109–116.